Journal of Aerosol Science 113 (2017) 85–94

Contents lists available at ScienceDirect

Journal of Aerosol Science

journal homepage: www.elsevier.com/locate/jaerosci

Investigation of alternative metrics to quantify PM mass emissions from light duty vehicles

Jian Xue[a,b], Yang Li[a,b], David Quiros[c], Shaohua Hu[c], Tao Huai[c], Alberto Ayala[c], Heejung S. Jung[a,b,*]

[a] Center for Environmental Research and Technology (CE-CERT), Bourns College of Engineering, University of California, Riverside, 1084 Columbia Ave, Riverside, CA, USA
[b] University of California Riverside, Department of Mechanical Engineering, 900 University Ave, Riverside, CA, USA
[c] California Air Resources Board (CARB), 1900 14th Street, Sacramento, CA 95814, USA

ARTICLE INFO

Keywords:
Solid particle number
Total particle number
Particle active surface area
Aerosol surface area
Black carbon
Suspend particle mass
Diffusion charger
Photoacoustic

ABSTRACT

We evaluated the performance of six alternative particulate matter (PM) metrics relative to the regulatory gravimetric method during chassis dynamometer testing of five light-duty vehicles over the Federal Test Procedure (FTP) and Supplemental FTP (US06) cycles. Alternative metrics included three mass-based metrics including black carbon (BC), two suspended PM mass using integrated particle size distribution (IPSD) method, and three number/surface-based metrics including total particle number (PN), solid particle number (SPN), and particle active surface area (PS). The results showed PM emissions over the FTP cycle were dominated by solid particles on a mass basis (BC to PM ratio = 0.6 ± 0.5), whereas over the US06 cycle were dominated by semi-volatile particles (BC to PM ratio = 0.2 ± 0.2). Moderate to strong correlations were reported between the gravimetric method and the six alternative metrics for FTP and US06 cycles separately (R^2 = 0.69–0.91), i.e. the best-fit lines were strongly dependent upon the cycle. On the other hand, the six alternative PM mass and number metrics exhibited moderate to strong correlations regardless of the test cycle (R^2 = 0.66–0.98). We attribute the observed cycle dependency between alternative metrics and the gravimetric mass method to the greater gravimetric sensitivity to organic and semi-volatile PM than for most alternative metrics.

1. Introduction

Particulate matter (PM) emitted from vehicles is associated with adverse health effects, including cardiovascular and pulmonary diseases (Donaldson, Li, & Macnee, 1998; EPA, 2002; Oberdorster et al., 2004). Regulations for vehicle PM emissions in the U.S. are based on gravimetric measurement of PM collected onto filter media as defined in Code of Federal Regulations (CFR) parts 1065 and 1066 (CFR, 2011, 2012). With the recent adoption of the Low Emission Vehicle (LEV) III emission standards in California, which

Abbreviations used in this study: ARB, California Air Resources Board; BC, black carbon; BET, Brunauer, Emmett and Teller; CFR, Code of Federal Regulations; CPC, condensation particle counter; CS, catalytic stripper; CVS, constant volume sampler; DMM, Dekati® mass monitor; DPF, diesel particulate filter; EAD, electric aerosol detector; EC, elemental carbon; EEPS, engine exhaust particle sizer; ELPI, electrical low pressure impactor; FTP, Federal Test Procedure; GDI, gasoline direct injection; GM, gravimetric mass; IPSD, Integrated Particle Size distribution; LDVs, light-duty vehicles; LEV III, Low Emissions Vehicle III program; MSS, micro soot sensor; MY, model year; NMHCs, Non-Methane Hydrocarbons Compounds; PFI, port-fuel injection; PM, particulate matter; PMP, Particle Measurement Program; PN, particle number; PS, particle surface area; PSD, particle size distribution; SI, supporting information; SPN, solid particle number

* Corresponding author at: Center for Environmental Research and Technology (CE-CERT), Bourns College of Engineering, University of California, Riverside, 1084 Columbia Ave, Riverside, CA, USA.
E-mail address: heejung@engr.ucr.edu (H.S. Jung).

http://dx.doi.org/10.1016/j.jaerosci.2017.07.021
Received 11 February 2017; Received in revised form 18 July 2017; Accepted 31 July 2017
Available online 01 August 2017
0021-8502/

includes a 1 mg/mi PM emissions standard for light-duty vehicles (LDVs) beginning in 2025, there have been many efforts designed to evaluate and improve the accuracy of the filter-based gravimetric method. One recent effort, the Coordinating Research Council (CRC) E-99 project, identified that increasing the filter face velocity (FFV) from 100 to 150 cm/s and combining multiple test phases onto fewer filters can improve the signal to noise ratio of the gravimetric method, without altering the measurement of PM. Using these recommendations as well as other standard operating practices, ARB demonstrated that the gravimetric filter-based method is suitable for measuring PM emissions from vehicles at levels well below 1 mg/mi (ARB, 2015). However, the gravimetric method reports composite PM emissions for the entirety of a test cycle, and does not provide real-time emissions data or other physiochemical characteristics of PM emissions. This information is helpful when conducting research and development, tracking the performance of new vehicle technologies, and also for developing new PM measurement methods for use in both the field and laboratory.

In 2011, the European Commission introduced a Solid Particle Number (SPN, $D_p > 23$ nm) limit PM emissions from LDVs in the framework of Particle Measurement Program (PMP). A study by Giechaskiel, Dilara, and Andersson (2008) showed SPN method measurement variability (~38%) was lower than the gravimetric method (~55%). Additionally, the evaluation demonstrated that SPN was sufficiently sensitive to distinguish between an empty and full fill state of a diesel particulate filter (DPF). However, by design, the SPN metric is insensitive to semi-volatile particles, which can be notable under certain conditions, such as during DPF regeneration (Dwyer et al., 2010). The particle number (PN) emissions rate is expected to be more variable than the SPN emission rate as it includes dilution-formed semi-volatile particles that are in constant flux between the gas and particle phase, and therefore dependent on dilution and engine operating conditions (Khalek, Kittelson, & Brear, 1999).

Other studies suggested active surface area measured with a diffusion charger (Pham and Jung, 2006; Jung & Kittelson, 2005; Mokhtar et al., 2013) or an epiphanimeter (Gini, Helmis, & Eleftheriadis, 2013; Pandis, Baltensperger, Wolfenbarger, & Seinfeld, 1991) could be a potential alternative metric for measuring PM from vehicle exhaust. Active surface area has been shown to be independent from PM chemical composition (Adachi, Kousaka, & Okuyama, 1985) and some studies have shown adverse heath effects were more associated with surface area than with mass or number (Brown, Collings, Harrison, Maynard, & Maynard, 2000; Stoeger et al., 2006; Tran et al., 2000). Although active surface area is different from surface area determined by Brunauer, Emmett and Teller (BET) technique (Brunauer, Emmett, & Teller, 1938), or geometric surface area, active surface area is regarded as the most feasible surface metric to be measured for routine monitoring (Pham and Jung, 2006).

Black carbon (BC) emissions from light-duty vehicles is targeted for control because it is a major constituent of total PM mass (Bahreini et al., 2015), has been linked with adverse health effects and climate change, and has been recently identified as a short-lived climate pollutant (ARB, 2016). Real-time BC emission from the LDVs had been measured with various instruments that were based on photo-acoustic or optical technologies (Kamboures et al., 2015; Xue et al., 2016a, 2016b). The results generally suggested BC comprised a higher fraction of PM from gasoline direct injection (GDI) vehicles (55–106%) than PM from port-fuel injection (PFI) vehicles (7–88%).

Maricq and Xu (2004) conceptualized the Integrated Particle Size Distribution (IPSD) metric, which is another metric to determine real-time PM mass by multiplying the particle volume concentration with the size-dependent particle effective density. Specifically, a study by Liu et al. (2009) showed suspended PM mass estimated with the IPSD metric agreed with gravimetric mass within 10–20% when testing heavy-duty diesel engines using the Engine Exhaust Particle Sizer (EEPS, TSI Incorporated, Shoreview, MN, USA). However, recent studies by Li et al. (2014) and Quiros and Zhang (2015) showed IPSD mass was persistently lower than the gravimetric mass by 37–75% over the Federal Test Procedure (FTP) cycle when 40 LDVs were tested using the same EEPS model.

Two studies have focused on evaluating some other alternative metrics with respect to regulatory gravimetric mass. Mohr, Lehmann, and Rutter (2005) evaluated 16 different particle measurement systems using a heavy-duty diesel vehicle during both steady-state and transient conditions and with different levels of PM emissions (with exhaust passing/not passing the PM after-treatment device). Their results showed aerosol instruments (which included instruments such as the Condensation Particle Counter (CPC), Electrical Low Pressure Impactor (ELPI) and, and diffusion chargers) showed a good correlation ($R^2 > 0.94$) with EC, while showing poor correlation ($R^2 < 0.57$) with gravimetric filter method. More recently, Maricq, Szente, Harwell, and Loos (2016) evaluated three real-time aerosol instruments (i.e. a Dekati® Mass Monitor (DMM), an EEPS (with the calculation of PM mass using IPSD method), and a Micro Soot Sensor (MSS)) using eight LDVs over 50 Federal Test Procedure (FTP) tests. The results showed good correlation between the real-time instruments and the gravimetric method at higher PM emission rates (> 3 mg/mile), while MSS under predicted $PM_{2.5}$ mass as it measures soot fraction only. At lower PM emission rates (< 3 mg/mile), however, the correlations between real-time instruments and gravimetric filter were weaker. The results of some studies may suggest that the variability in the gravimetric method below 3 mg/mi is the cause (Maricq et al., 2016), whereas other studies have shown strong correlations between gravimetric and alternative metrics down to 0.2 mg/mi (Quiros & Zhang, 2015). Other work has specifically shown that suspended PM mass (IPSD) measured by the EEPS and BC mass were highly correlated for several LDVs equipped with different technologies when evaluated over the FTP cycle, where IPSD and BC mass accounted for only one-third of gravimetric PM mass for gasoline PFI vehicles, while a one-to-one relationship was obtained for GDI vehicles (Xue et al., 2016b).

In this paper, we present the PM emission rates as determined by additional four approaches in addition to the IPSD and BC mass presented by (Xue et al., 2016b). In aggregate, we present suspended PM mass measured by a DMM and IPSD mass from EEPS size distributions, total particle number (PN), solid particle number (SPN), and particle active surface area (PS). Comparisons are made over both the FTP and US06 cycles to evaluate a wide range of PM emissions scenarios associated with the standard and supplemental certification cycles. The goal of this study is to investigate the inter-correlation of all six alternative metrics, and the impact of driving conditions on their relationships relative to the regulatory filter-based gravimetric method.

2. Experimental

2.1. Measurement metrics

Table S1 lists all instruments and measurement metrics evaluated in this study.

2.1.1. Gravimetric mass (GM)

Gravimetric filter samples were drawn directly from the CVS tunnel, as shown in Fig. S1 in SI. Gravimetric PM mass was collected on 47 mm Whatman PTFE®-membrane filter with pore size of 2 μm. A single filter was used over both FTP and US06 cycles and PM was collected at typical room temperature of 23 ± 3 °C. The filter face velocity was maintained at 100 cm/s, consistent with CFR Part 1065, but other provisions of CFR Part 1065, such as controlling of the temperature at the filter face to 47 ± 5 °C and weighting flow rate for individual FTP phase, were not implemented. The typical weighting factors for each phase of FTP cycle were not used in this study to allow a direct comparison to the alternative metrics. Tunnel blanks were collected 12 times periodically during data collection.

2.1.2. Black Carbon (BC) measured by the photo-acoustic MSS

The emission rate of BC was measured by MSS (model 483) manufactured by AVL. The MSS is based on the photo-acoustic method and only sensitive to light-absorbing components (i.e. soot particles in the vehicle exhaust). MSS was calibrated by the manufacturer with filter-collected PM standard that was composed of at least 95% elemental carbon (EC) (Kasper, 2009). Our historical data showed the measurement of MSS agreed with the EC concentration measured by traditional thermal-optical analysis method (Wu, Ng, Huang, Wu, & Yu, 2012) within 13% with $R^2 = 0.94$ as shown in Fig. S2 in SI.

2.1.3. Suspended PM mass by EEPS ($IPSD_{EEPS}$)

The EEPS (Model 3090, firmware version 3.11, TSI Inc.) was used to measure particle size distribution. An EEPS uses a unipolar charger to induce a high degree of charge onto particles which are subsequently classified by their electrical mobility (Biskos, Reavell, & Collings, 2005; Mirme, 1994). The measured electrometer currents are inverted to particle size distributions into 32 bins (from 5.6 to 560 nm) with a newly developed inversion matrix for vehicle exhaust (known as Soot Matrix) (Wang et al., 2016; Xue et al., 2015). Number-based size distributions are converted into mass distributions with a size-dependent effective density function. This effective density function was obtained by fitting the data reported in Maricq and Xu (2004) and Quiros et al. (2015b) using a power fitting model Quiros et al. (2015b).

2.1.4. Suspended PM mass by DMM ($IPSD_{DMM}$)

The DMM directly reports PM mass for particles with aerodynamic diameters less than 1.2 μm using an electrical mobility channel, six aerodynamic channels, and a real-time estimate of particle effective density with a fixed mass-mobility scaling exponent (DEKATI, 2014; Virtanen et al., 2002). In the DMM, particles are charged by a corona discharge, then pass through an electrical mobility analyzer where the mobility diameter of the smallest particles ($d_p < 30$ nm) is determined (Lehmann, Niemela, & Mohr, 2004). Subsequently, particles enter a six-stage cascade impactor where the particles are classified based on their aerodynamic size. Because the DMM integrates mass over multiple size bins and reports a total suspended PM mass – similar to the IPSD method using the EEPS, we report DMM mass emissions as $IPSD_{DMM}$; however, no further processing was conducted beyond the directly-reported mass value by the DMM. It should be noted that the density measurement principle of DMM requires the measured particle size distribution to be unimodal, and that the DMM mass may be subject to uncertainty when measuring mass of multimodal size distributions.

2.1.5. Total Particle Number (PN)

The emission rate of particle number was originally designed to be measured by an ultrafine CPC (model 3776, TSI Inc.) which sampled from a secondary dilution tunnel with a dilution ratio set to either 3.9 or 8.8. The CPC has a lower cutoff diameter of 2.5 nm (d_{50}). However, during some of the tests, the number concentration of particles exceeded the maximum concentration limit of the CPC ($3{\cdot}10^5/cm^3$) indicating that a greater total dilution ratio would have been needed to keep the instrument within range. Therefore, the PN reported in this study was determined as the sum of the EEPS channels ($n = 32$, 5.6–560 nm). A previous study (Zervas and Dorlhène, 2006) showed the EEPS and a reference CPC agreed well when measuring PN emissions from a diesel engine, and we show a similar trend was generally observed in this study where total PN concentration was below $3{\cdot}10^5/cm^3$ ($R^2 = 0.96$ and slope = 0.93, Fig. S3 in SI).

2.1.6. Solid Particle Number (SPN)

A second unit of the same CPC 3776 model was used to measure SPN emissions. This CPC sampled from a second dilution tunnel (providing either 3.9 or 8.8 times additional dilution) and was equipped with a catalytic stripper (CS) upstream. The CS was operated at 300 °C to remove semi-volatile particles, and additionally by virtue of its design, particles with diameters less than 30 nm did not pass through the system. Therefore, in effect, the CS-CPC system used to measure SPN had an effective lower cutoff diameter (d_{50}) of 30 nm, although the CPC 3766 itself had a d_{50} of 2.5 nm. The d_{50} of the CS-CPC system is slightly larger than the d_{50} of the PMP system (23 nm), suggesting the SPN measured by the CS-CPS may be lower than that measured by the PMP system. According to Swanson, Kittelson, Watts, Gladis, and Twigg (2009), majority of the vehicle exhaust PM with diameter smaller than 30 nm is semi-

volatile in nature and will be removed by upstream thermal treatment. However, there is a chance of contribution of sub 30 nm solid particles to SPN count in non-negligible amount, in particular under low load conditions for which high concentrations of soli particles in the 20 nm range have been observed (Giechaskiel et al., 2014 and the references therein). Under these conditions, the CS-CPC system likely provides lower measurement of SPN as a PMP-compliant system.

2.1.7. Particle active surface area (PS)

A diffusion charger, Electric Aerosol Detector (EAD, modal 3070A, TSI), was used to measure particle active surface area. The response of EAD is proportional to $d^{1.13}$ for the size range from 10 nm to 1 μm (TSI, 2012), while TSI truncated 1.13 to 1 in the display and output of the instrument and presents it as a particle length unit. This arbitrary truncation of the exponent makes non-expert users think that the instrument responds to the particle length unit. However this instrument actually responds to active or Fuchs surface area of particles. The exponent 1.13 is due to the inclusion of transition regimes in the instrument's 10 nm to 1 μm size range. More details about the instrument were given in Jung and Kittelson (2005). The active surface is fraction of the geometrical surface area of particles that is responsible for mass transfer of diffusing ions, which is also known as the Fuchs surface. This other portion of geometrical surface area that is not measured by the EAD is the passive surface, which includes inner surfaces, and surfaces in bays or cracks, or for larger particles, the surfaces around the front and back dead center of the laminar flow (Keller, Fierz, Siegmann, Siegmann, & Filippov, 2001).

2.1.8. Gaseous criteria pollutant emissions

In addition, bag emission for total hydrocarbons, non-methane hydrocarbon (NMHC), CO, CO_2, and NO_x were measured with a Horiba MEXA-7200D Automotive Emissions Analyzer System and where necessary, the appropriate CFR corrections were applied for analyzer drift, intake-air humidity, and dry-to-wet conversions.

2.2. Test cell and driving cycles

All tests were conducted at the University of California, Riverside Center for Environmental Research (CE-CERT) Vehicle Emissions Research Laboratory (VERL). The facility is equipped with a Burke E. Porter 48-inch single barrel light duty dynamometer. Vehicle exhaust pipe was fully connected to the Constant Volume System (CVS). The CVS was operated at 9–15 m^3/min, creating 18–28 times primary dilution during the FTP cycle, and 11–14 times primary dilution during the US06 tests.

Vehicles were tested over two regulated driving cycles, the FTP and the Supplemental FTP cycle (US06). The FTP (average speed is 34.12 km/h) is the primary emission certification test for all LDVs in the U.S., and is designed to represent city driving conditions. This cycle comprises three phases, a “cold start” phase, a “stabilized” phase and a “hot start” phase. There is a 10 min “hot soak period” between the “stabilized” phase and the “hot start” phase. The US06 cycle (average speed equals 77.9 km/h) represents more aggressive driving behavior. It includes high speed, high acceleration, and rapid speed fluctuations. The speed time traces for the FTP and the US06 cycles are presented Fig. S4 in SI.

2.3. Test vehicles and fuels

Five vehicles were tested in this study, including four GDI vehicles and one PFI vehicle. These vehicles included a 2012 Mazda 3 (denoted as GDI-1), a 2009 VW Tiguan (denoted as GDI-2), a 2012 Mercedes Benz E350 coupe (denoted as GDI-3), a 2012 Kia Optima

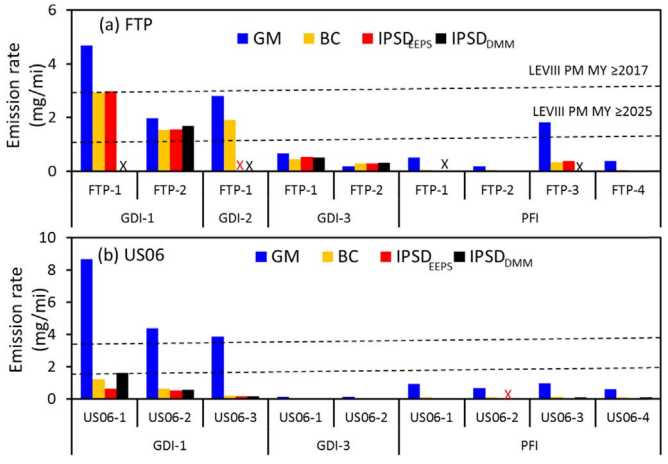

Fig. 1. Emission rate of PM over (a) FTP cycle and (b) US06 cycle for the mass-related metrics. “X” indicates the measurement is not available for this test. The dashed lines represent LEVIII emission standard beginning with MY 2017 (3 mg/mile) and 2025 (1 mg/mile), respectively. Data smaller than method detection limit (MDL) (Table S4) were replaced by ½ MDL. The 3rd and 4th FTP tests with GDI-1 and the FTP test with GDI-4 (Table S3) were not presented in this figure due to limited metrics availabilities.

(Denoted as GDI-4) and a 2012 Nissan Versa (denoted as PFI). This selection of gasoline PFI and GDI vehicles provides a wide range of PM emissions from LDVs. Vehicle specifications are summarized in Table S2 in SI.

3. Results and discussion

3.1. Emission rates

Fig. 1 shows PM emission rates determined by the mass-based metrics for the individual FTP tests (Fig. 1a) and US06 tests (Fig. 1b) with each vehicle. The data used to plot Fig. 1 are presented in Table S3 in SI. As it was shown in Fig. 1, PM mass emission rates varies by vehicle technologies.

For the FTP tests, the two wall-guided GDI vehicles (GDI-1 and GDI-2) had high PM emission rates, varying from ~2 to ~4.5 mg/mi with gravimetric method, while other vehicles generally had PM emission rates lower than 1 mg/mi. The BC emission rates were generally lower than those measured by gravimetric method except the test of FTP-2 with vehicle GDI-3 for which the total mass collected on the PTFE filter was only 12 μg, close to the tunnel blank loading (8 μg). However, the ratio between BC and gravimetric mass, varied significantly among the vehicles. The BC accounted for 69 ± 6% and 15 ± 4% of gravimetric mass with the GDI and PFI vehicles, respectively. The $IPSD_{EEPS}$ accounted for 91 ± 24% of GM with the GDI vehicles, but only accounted for 12 ± 11% of GM with the PFI vehicles. Similarly, the $IPSD_{DMM}$ accounted for 81 ± 7% of gravimetric mass with the GDI vehicles, only for ~5% of gravimetric mass with the PFI vehicle. High correlation (R^2 = 1.00) was found between two IPSD PM masses, with $IPSD_{DMM}$ slightly exceeded $IPSD_{EEPS}$ by 8% (Fig. S5 in SI).

Fig. 1(b) shows the relative response of the alternative metrics during the US06 cycle; the vehicles always had higher gravimetric mass compared to alternative metrics. Compared to FTP tests, BC accounted for even less of the gravimetric mass over the US06 tests, with 27 ± 23% for the tests with GDI vehicles and 13 ± 3% for the tests with PFI vehicle. These results indicate PM emission from the US06 cycles were more dominated by semi-volatile particles compared with PM emissions from the FTP cycle. Similarly, $IPSD_{EEPS}$ and $IPSD_{DMM}$ account for only 13 ± 10% of the gravimetric mass, even with the GDI vehicles (for which $IPSD_{EEPS}$ and $IPSD_{DMM}$ account for 17 ± 12% of gravimetric mass mass).

Fig. 2 presents number/surface-based metrics. SPN (> 30 nm) accounted 8% of total PN over both FTP and US06 cycles. Geometric mean diameters were obtained using PS/PN ratio following the method by Pham and Jung (2016). For GDI vehicles, geometric mean diameter tends to be larger over FTP cycle compared to US06, while it was not distinguishable for PFI vehicles between two types of cycles (Fig. S6 in SI).

3.2. Correlations between the metrics

Fig. 3 contains scatter plots presenting the alternative metrics versus the reference gravimetric mass. The dashed red and blue lines represent the linear regression of the FTP and US06 tests, respectively. The inset figures show the correlations for the tests with emission rates less than 1 mg/mile for the gravimetric method. The same figure was plotted in log-scale in Fig. S7 in SI.

Fig. 3 shows when fitting a linear curve to FTP and US06 tests, good correlations between the gravimetric mass and the alternative metrics are achieved over two cycles separately, with R^2 varying from 0.85 to 0.94 over the FTP cycle and 0.79–0.92 over the US06 cycle. Interestingly, the slopes for the regression lines are 66–88% lower for the US06 tests when compared with those for the FTP tests, indicating the discrepancies between alternative metrics and gravimetric mass over the US06 tests are much more significant than those over the FTP cycles.

One possible explanation of the cycle-dependent correlation is hydrocarbon emissions are higher during US06 than FTP tests, and the fraction of hydrocarbons with lower volatility may partition into the particulate phase and become entrained onto filter media, but are not detected as adequately by our real-time measures of suspended PM mass. Fig. 4 shows average NMHC concentrations in

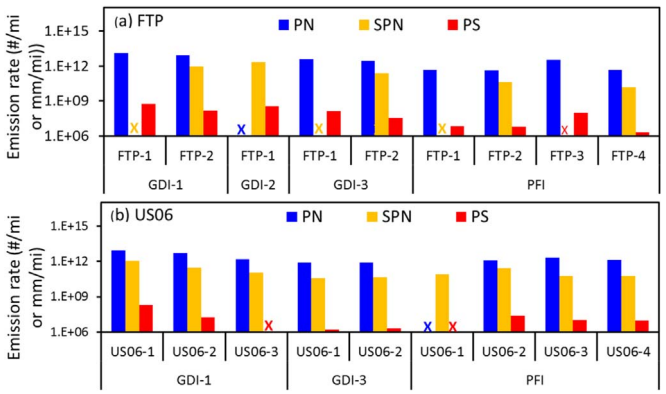

Fig. 2. Absolute emission rate of PM over (a) FTP cycle and (b) US06 cycle for the number/surface-related metrics. "X" indicates the measurement is not available for this test.

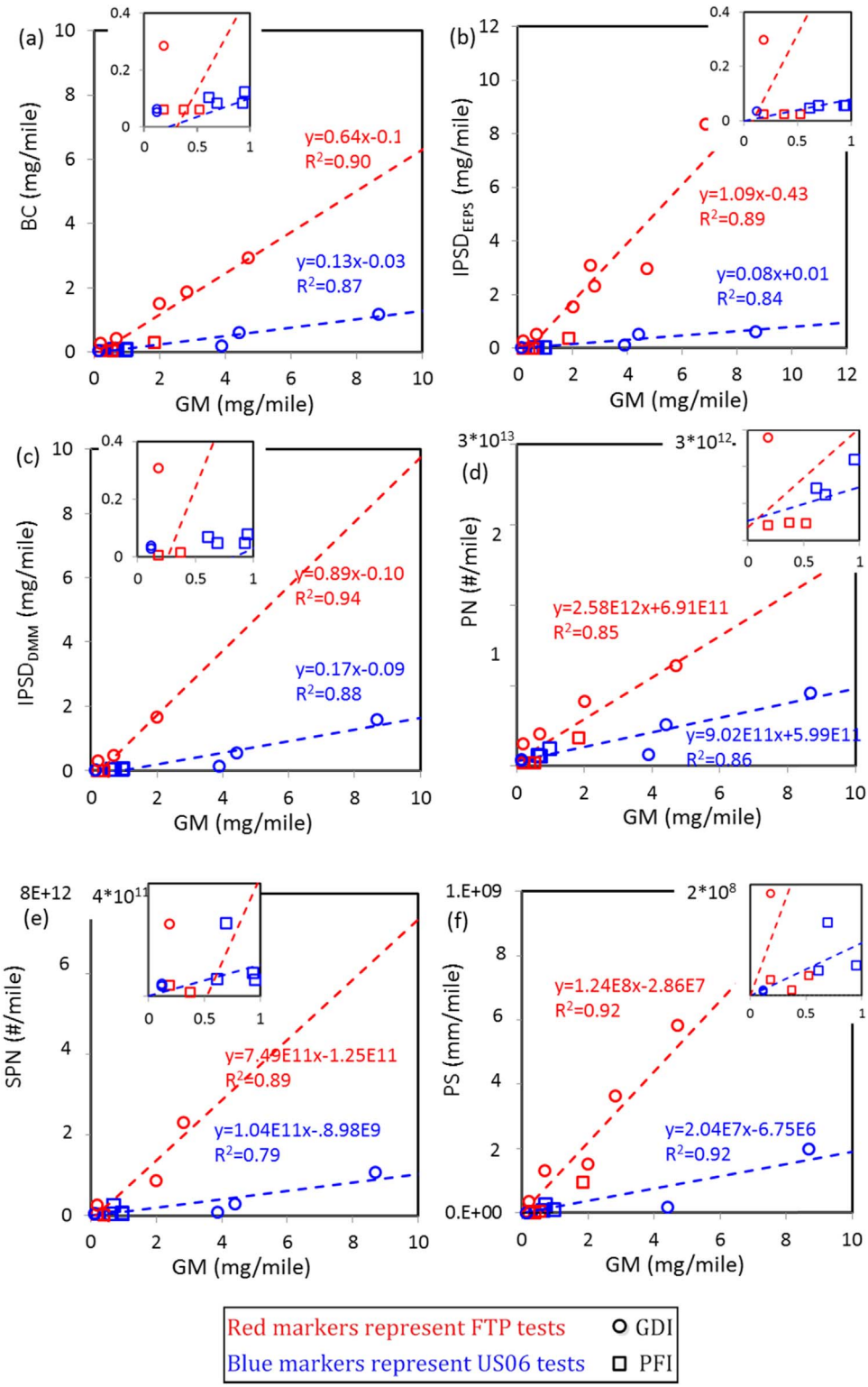

Fig. 3. Correlations between alternative metrics and referenced GM method. The correlations were studied with FTP test and US06 tests separately. (a) BC vs. GM; (b) $IPSD_{EEPS}$ vs. GM; (c) $IPSD_{DMM}$ vs. GM; (d) PN vs. GM; (e) SPN vs. GM; (f) PS vs. GM.

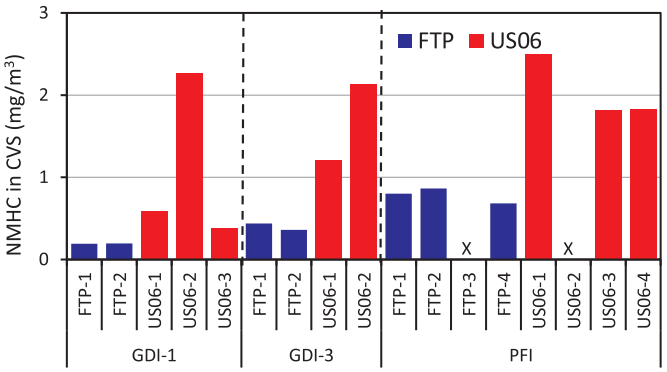

Fig. 4. Comparison between the Non-Methane Hydrocarbon Compounds (NMHCs) in the CVS during FTP tests and US06 test for each vehicle. Vehicle GDI-2 and GDI-4 don't have US06 test, so they are omitted in the figure.

the CVS over the US06 cycle was up to ten times higher than concentrations measured over the FTP cycle. Additionally, during FTP tests, 80–99% of the NMHC was emitted during the first phase of FTP cycle, and therefore it is possible that semi-volatile PM collected during the first phase may have been desorbed in subsequent phases with lower NMHC concentrations. Therefore, elevated gas-phase concentrations emitted over the US06 cycle may have contributed to higher gravimetric PM measurements relative to the alternative mass metrics evaluated.

Filter adsorption artifact is thought to be by either adhesion of organic gas molecules or adsorption of particle converted from gas onto the filter media. The contribution of mass by each mechanism is subject to multiple parameters such as filter face velocity, filter/gas temperature, soot loading etc (Högström et al., 2012). Chase et al. (2004) studied the effect of filter media and temperature on filter adsorption artifact for the measurement of vehicle PM emissions. While the effect of filter media was easily found, the effect of filter temperature was not (See their Figure 7). Additionally, when controlling the temperature of gravimetric filter media to CFR 1065 specifications (47 ± 5 °C) with a dataset of hundreds of tests for several vehicles in multiple test cells, the same cycle-dependent correlations between gravimetric and alternative metrics were obtained (Quiros & Zhang, 2015). Henceforth, the lack of temperature control in our study may have positively favored the collection of some semi-volatile materials onto filters, but we conclude that any impact only marginally impacted the measured values and does not impact the conclusions of the work.

Uncertainty associated with applying static particle effectively densities for the IPSD method may always be a possible source of uncertainty in estimating PM mass emissions from mobility-based size distributions (Quiros et al., 2015b; Xue et al., 2016). Previous studies identified up to a 20% potential uncertainties associated with using effective density functions derived using different experimental methods (instrumentation and duty cycles), test vehicles (PFI, GDI, light-duty diesel vehicles with DPF, and heavy-duty diesel engines with DPFs), and fitting approaches (exponential vs. power fit) (Liu et al., 2009; Quiros et al., 2015b; Xue et al., 2016b). The DMM measures particulate effective density in real time, and if successful, could reduce some of the uncertainty associated with transient test cycles. However, as mentioned above, the density measurement method a DMM adopts requires a unimodal particle size distribution, and if particles are bimodal, the density measurement fails and the PM mass concentration is calculated assuming unit density (1 g/cm^3).

The strong observed correlations between alternative metrics and gravimetric mass suggest that adopting strategies to control gravimetric mass may incidentally reduce the signal from any other metric of suspended PM. The slopes of the linear regressions indicated to reduce 1 mg/mile emission of gravimetric mass may respectively reduce 0.64 mg/mile, ~1 mg/mile, 2.58*10^{12} #/mile, 7.49*10^{11} #/mile and 1.24*10^8 mm/mile emissions for BC, suspended PM mass, PN, SPN and PS over the FTP tests. Over the US06 cycle, since the slopes were smaller, reduction of 0.13 mg/mile, ~0.1 mg/mile, 9.02*10^{11} #/mile, 1.04*10^{11} #/mile and 2.04*10^7 mm/mile of PM emission will be benefited for BC, suspended PM mass, PN, SPN and PS, respectively, by reducing per mg/mile gravimetric mass emission.

We report these reductions for the FTP and US06 cycles separately because distinctly different trends were observed for the relationship to gravimetric to alternative PM metrics (Fig. 5). When pooling FTP and US06 cycles, correlations between alternative vs. gravimetric PM mass were medium to poor (R^2 varying from 0.21 to 0.54, Table 1); however the pooled data showed strong inter-correlation among alternative metrics themselves (R^2 varying from 0.65 to 0.99, Table 1). Fig. 5 presents scatter plots of both FTP and US06 test data for all alternative metrics versus particle surface and shows good correlations over a wide range of emission factors (R^2 varying from 0.79 to 0.99). Importantly, as indicated by the inset figures, strong linear relationships were maintained for tests with PM mass emissions below 1 mg/mile, and the best-fit lines nearly pass through the origin, indicating metric equivalency at near-zero emissions levels. One exception was a slight positive y-intercept on the plot of total PN vs. PS, which was likely because high background noise of EEPS compared to EAD measurement.

4. Conclusions

This paper evaluated three alternative mass-based metrics including BC using a MSS, suspended PM using an EEPS, and suspended PM mass using a DMM; and three number/surface-based metrics including total PN, SPN, and active PS area. We reported strong

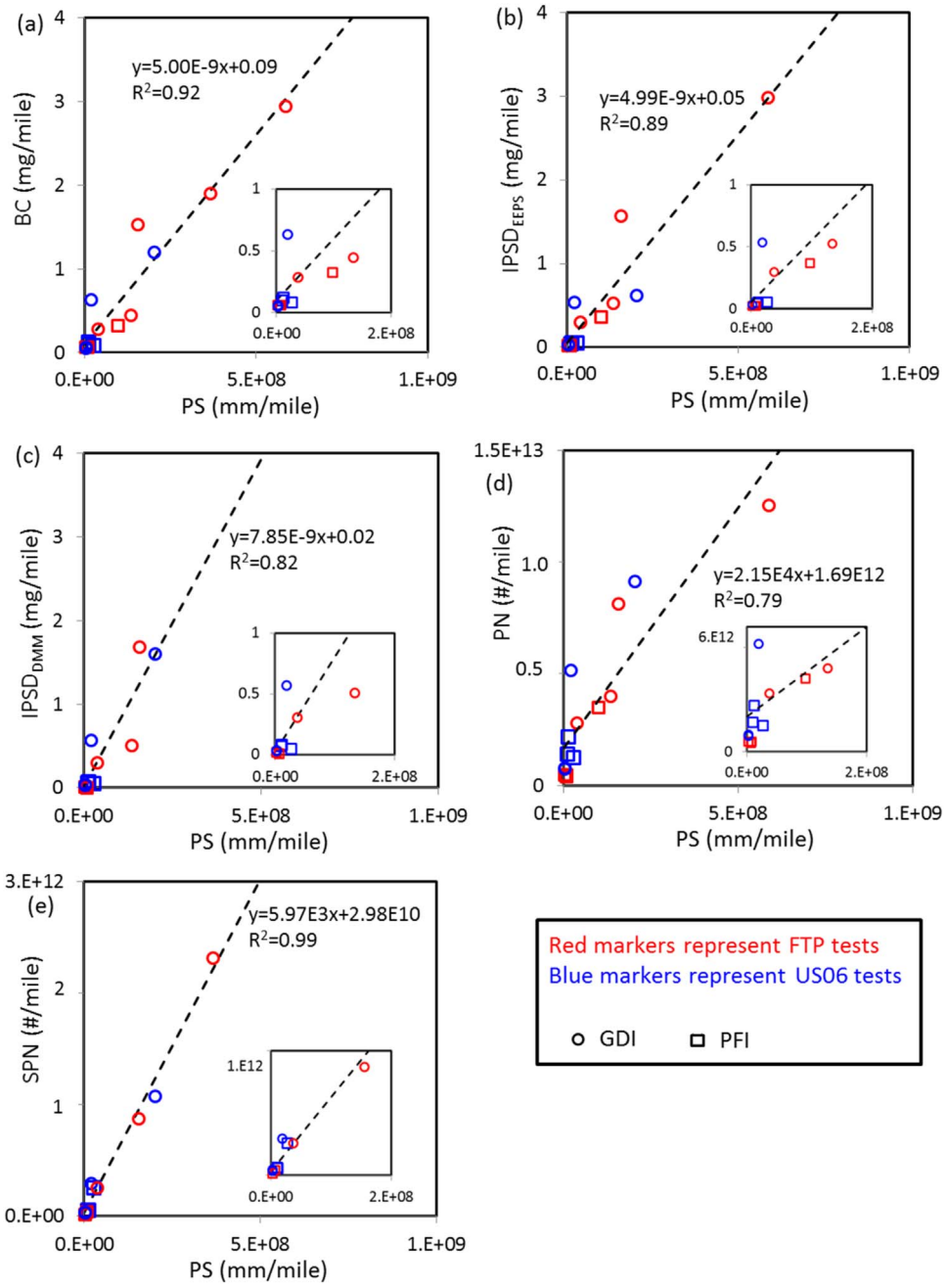

Fig. 5. Correlations between alternative metrics and PS. FTP and US06 tests were put together to study the correlations. (a) BC vs. PS; (b) $IPSD_{EEPS}$ vs. PS; (c) $IPSD_{DMM}$ vs. PS; (d) PN vs. PS; (e) SPN vs. PS.

inter-correlations among these six alternative metrics, suggesting that adopting strategies to control one parameter may incidentally reduce the signal from any other metric of suspended PM. Additionally the relationship among the six alternative metrics remained relative robust to driving cycle and did not exhibit different responses between the FTP and US06 driving cycles. The outcomes demonstrate that the alternative metrics, provided by instruments adopting different measurement principles, agree among each other regardless of the testing cycles. On the other hand, we found correlations between gravimetric mass and alternative metrics were cycle dependent. We attribute the observed cycle dependency between alternative metrics and gravimetric mass to greater gravimetric sensitivity to organic and semi-volatile PM collection than for most alternative metrics. We note the conclusion is made based on the current set of data, more measurement is necessary to further elucidate the result in the future study.

Table 1
Slope and R^2 of linear regression between the metrics investigated in this study.

	GM	PN	SPN	PS	BC	$IPSD_{EEPS}$	$IPSD_{DMM}$
GM							
PN	4.8E-13(0.54)*						
SPN	1.8E-12(0.22)	8.2E+00(**0.91**)#					
PS	8.1E-09(0.32)	2.2E+04(**0.79**)	6.0E+03(**0.99**)				
BC	1.7E+00(0.35)	4.4E+12(**0.91**)	9.6E+11(**0.87**)	1.8E+08(**0.92**)			
$IPSD_{EEPS}$	1.4E+00(0.21)	4.8E+12(**0.81**)	6.2E+11(**0.65**)	1.8E+08(**0.89**)	9.8E-01(**0.96**)		
$IPSD_{DMM}$	2.9E+00(0.46)	4.8E+12(**0.95**)	5.6E+11(**0.94**)	1.1E+08(**0.82**)	8.1E-01(**0.98**)	6.8E−01(**0.81**)	

* :R^2 is in the parentheses. Values larger than 0.64 (R = 0.8) are bolded.

Acknowledgement

This program was supported by the California Air Resources Board under contract 11–548.

Appendix A. Supporting information

Supplementary data associated with this article can be found in the online version at http://dx.doi.org/10.1016/j.jaerosci.2017.07.021.

References

Adachi, M., Kousaka, Y., & Okuyama, K. (1985). Unipolar and bipolar diffusion charging of ultrafine aerosol-particles. *Journal of Aerosol Science*, *16*(2), 109–123. http://dx.doi.org/10.1016/0021-8502(85)90079-5.

ARB (2015). An update on the measurement of PM emissions at LEV III levels. Available at 〈https://www.arb.ca.gov/msprog/levprog/leviii/lev_iii_pm_measurement_feasibility_tsd_20151008.pdf〉.

ARB (2016). Revised proposed short-lived climate pollutant reduction strategy. Available at: 〈https://www.arb.ca.gov/cc/shortlived/meetings/11282016/revisedproposedslcp.pdf〉.

Bahreini, R., Xue, J., Johnson, K., Durbin, T., Quiros, D., Hu, S., & Jung, H. (2015). Characterizing emissions and optical properties of particulate matter from PFI and GDI light-duty gasoline vehicles. *Journal of Aerosol Science*, *90*, 144–153. http://dx.doi.org/10.1016/j.jaerosci.2015.08.011.

Biskos, G., Reavell, K., & Collings, N. (2005). Description and theoretical analysis of a differential mobility spectrometer. *Aerosol Science and Technology*, *39*(6), 527–541.

Brown, L. M., Collings, N., Harrison, R. M., Maynard, A. D., & Maynard, R. L. (2000). Ultrafine particles in the atmosphere: Introduction. *Philosophical Transactions of the Royal Society of London Series a-Mathematical Physical and Engineering Sciences*, *358*(1775), 2563–2565.

Brunauer, S., Emmett, P. H., & Teller, E. (1938). Adsorption of gases in multimolecular layers. *Journal of the American Chemical Society*, *60*, 309–319. http://dx.doi.org/10.1021/Ja01269a023.

CFR (2011). Code of federal regulations, 40 Parts, PART 1065—ENGINE-TESTING PROCEDURES. 〈http://www.ecfr.gov/cgi-bin/text-idx?Tpl=/ecfrbrowse/Title40/40cfr1065_main_02.tpl〉.

CFR (2012). Code of Federal Regulations, 40 Parts, PART 1066—VEHICLE-TESTING PROCEDURES. 〈http://www.ecfr.gov/cgi-bin/text-idx?Tpl=/ecfrbrowse/Title40/40cfr1066_main_02.tpl〉.

Chase, R. E., Duszkiewicz, G. J., Richert, J. F. O., Lewis, D., Maricq, M. M., & Xu, N. (2004). *PM measurement artifact: Organic vapor deposition on different filter media*. SAE Technical Paper Series (2004-01-0967).

DEKATI (2014). Dekati Mass Monitor DMM. Available at: 〈http://www.particleinstruments.com/sites/default/files/pdfs/dmm.pdf〉.

Donaldson, K., Li, X. Y., & Macnee, W. (1998). Ultrafine (nanometre) particle mediated lung injury. *Journal of Aerosol Science*, *29*(5–6), 553–560.

Dwyer, H., Ayala, A., Zhang, S., Collins, J., Huai, T., Herner, J., & Chau, W. (2010). Emissions from a diesel car during regeneration of an active diesel particulate filter. *Journal of Aerosol Science*, *41*(6), 541–552. http://dx.doi.org/10.1016/j.jaerosci.2010.04.001.

EPA (2002). Health Assessment document for diesel engine exhaust. In United States Environmental Protection Agency, EPA/600/8-90/057F; US EPA: Washington, DC, Available at: 〈http://cfpub.epa.gov/ncea/cfm/recordisplay.cfm?Deid=29060#Download〉.

Giechaskiel, B., Dilara, P., & Andersson, J. (2008). Particle measurement programme (PMP) light-duty inter-laboratory exercise: Repeatability and reproducibility of the particle number method. *Aerosol Science and Technology*, *42*(7), 528–543. http://dx.doi.org/10.1080/02786820802220241.

Giechaskiel, B., Maricq, M. M., Ntziachristos, L., Dardiotis, C., Wang, X. L., Axmann, H., & Schindler, W. (2014). Review of motor vehicle particulate emissions sampling and measurement: From smoke and filter mass to particle number. *Journal of Aerosol Science*, *67*, 48–86.

Gini, M. I., Helmis, C. G., & Eleftheriadis, K. (2013). Cascade Epiphaniometer: An instrument for aerosol "Fuchs" surface area size distribution measurements. *Journal of Aerosol Science*, *63*, 87–102. http://dx.doi.org/10.1016/j.jaerosci.2013.05.001.

Högström, R., Karjalainen, P., Ojanperä, J. Y., Rostedt, A., Heinonen, M., Mäkelä, J. M., & Keskinen, J. (2012). Study of the PM gas-phase filter artifact using a setup for mixing diesel-like soot and hydrocarbons. *Aerosol Science and Technology*, *46*(9), 1045–1052.

Jung, H. J., & Kittelson, D. B. (2005). Characterization of aerosol surface instruments in transition regime. *Aerosol Science and Technology*, *39*(9), 902–911. http://dx.doi.org/10.1080/02786820500295701.

Kamboures, M. A., Rieger, P. L., Zhang, S., Sardar, S. B., Chang, M. C. O., Huang, S. M., & Ayala, A. (2015). Evaluation of a method for measuring vehicular PM with a composite filter and a real-time BC instrument. *Atmospheric Environment*, *123*, 63–71. http://dx.doi.org/10.1016/j.atmosenv.2015.10.061.

Kasper, M. (2009). CAST-Combustion aerosol standard: principle and new applications. Available at: 〈http://www.sootgenerator.com/documents/Kasper.pdf〉.

Keller, A., Fierz, M., Siegmann, K., Siegmann, H. C., & Filippov, A. (2001). Surface science with nanosized particles in a carrier gas. *Journal of Vacuum Science & Technology a-Vacuum Surfaces and Films*, *19*(1), 1–8. http://dx.doi.org/10.1116/1.1339832.

Khalek, A., Kittelson, D. B., & Brear, F. (1999). *The influence of dilution conditions on diesel exhaust particle size distribution measurements*. SAE Technical Paper (1999-01-1142)(10.4271/1999-01-1142).

Lehmann, U., Niemela, V., & Mohr, M. (2004). New method for time-resolved diesel engine exhaust particle mass measurement. *Environmental Science & Technology*, *38*(21), 5704–5711. http://dx.doi.org/10.1021/es035206p.

Li, Y., Xue, J., Johnson, J. P., Durbin, T. D., Villeta, M., Pham, L., & Ayala, A. (2014). *Determination of suspended exhaust PM mass for light-duty vehicles*. SAE Technical Paperhttp://dx.doi.org/10.4271/2014-01-1594.

Liu, Z. G., Vasys, V. N., Dettmann, M. E., Schauer, J. J., Kittelson, D. B., & Swanson, J. (2009). Comparison of strategies for the measurement of mass emissions from

diesel engines emitting ultra-low levels of particulate matter. *Aerosol Science and Technology*, *42*(11), 1142–1152. http://dx.doi.org/10.1080/02786820903219035.

Maricq, M. M., Szente, J. J., Harwell, A. L., & Loos, M. J. (2016). How well can aerosol instruments measure particulate mass and solid particle number in engine exhaust? *Aerosol Science and Technology*, *50*(6), 605–614. http://dx.doi.org/10.1080/02786826.2016.1169244.

Maricq, M. M., & Xu, N. (2004). The effective density and fractal dimension of soot particles from premixed flames and motor vehicle exhaust. *Journal of Aerosol Science*, *35*(10), 1251–1274.

Mirme, A. (1994). *Electric aerosol spectrometry (Doctoral thesis)*. Tartu, Estonia: Tartu University.

Mohr, M., Lehmann, U., & Rutter, J. (2005). Comparison of mass-based and non-mass-based particle measurement systems for ultra-low emissions from automotive sources. *Environmental Science & Technology*, *39*(7), 2229–2238. http://dx.doi.org/10.1021/es049550d.

Mokhtar, M. A., Jayaratne, R., Morawska, L., Mazaheri, M., Surawski, N., & Buonanno, G. (2013). NSAM-derived total surface area versus SMPS-derived "mobility equivalent" surface area for different environmentally relevant aerosols. *Journal of Aerosol Science*, *66*, 1–11. http://dx.doi.org/10.1016/j.jaerosci.2013.08.003.

Oberdorster, G., Sharp, Z., Atudorei, V., Elder, A., Gelein, R., Kreyling, W., & Cox, C. (2004). Translocation of inhaled ultrafine particles to the brain. *Inhalation Toxicology*, *16*(6–7), 437–445.

Pandis, S. N., Baltensperger, U., Wolfenbarger, J. K., & Seinfeld, J. H. (1991). Inversion of aerosol data from the Epiphaniometer. *Journal of Aerosol Science*, *22*(4), 417–428. http://dx.doi.org/10.1016/0021-8502(91)90002-Y.

Pham, L., & Jung, H. J. (2016). Alternative metrics for spatially and temporally resolved ambient particle monitoring. *Journal of Aerosol Science*, *102*, 96–104.

Quiros, D. C., Zhang, S., Sardar, S., Kamboures, M. A., Eiges, D., Zhang, M., & Hu, S. H. (2015a). Measuring particulate emissions of light duty passenger vehicles using Integrated Particle Size Distribution (IPSD). *Environmental Science and Technology*, *49*(9), 5618–5627.

Quiros, D. C., Hu, S. H., Hu, S. S., Lee, E. S., Sardar, S., Wang, X. L., & Huai, T. (2015b). Particle effective density and mass during steady-state operation of GDI, PFI, and diesel passenger cars. *Aerosol Science and Technology*, *83*, 39–54.

Stoeger, T., Reinhard, C., Takenaka, S., Schroeppel, A., Karg, E., Ritter, B., & Schulz, H. (2006). Instillation of six different ultrafine carbon particles indicates a surface area threshold dose for acute lung inflammation in mice. *Environmental Health Perspectives*, *114*(3), 328–333. http://dx.doi.org/10.1289/ehp.8266.

Swanson, J. J., Kittelson, D. B., Watts, W. F., Gladis, D. D., & Twigg, M. V. (2009). Influence of storage and release on particle emissions from new and used CRTs. *Atmospheric Environment*, *43*(26), 3998–4004. http://dx.doi.org/10.1016/j.atmosenv.2009.05.019.

Tran, C. L., Buchanan, D., Cullen, R. T., Searl, A., Jones, A. D., & Donaldson, K. (2000). Inhalation of poorly soluble particles. II. Influence of particle surface area on inflammation and clearance. *Inhalation Toxicology*, *12*(12), 1113–1126. http://dx.doi.org/10.1080/08958370050166796.

TSI (2012). Electrical aerosol detector model 3070A: A fast aerosol concentration detector for wide dynamic range. Available at: ⟨http://www.tsi.com/uploadedFiles/_Site_Root/Products/Literature/Spec_Sheets/3070A.pdf⟩.

Virtanen, A., Ristimaki, J., Marjamaki, M., Vaaraslahti, K., Keskinen, J., & Lappi, M. (2002). *Effective density of diesel exhaust particles as a function of size*. SAE technical paper (2002-01-0056).

Wang, X. L., Grose, M. A., Caldow, R., Osmondson, B. L., Swanson, J. J., Chow, J. C., & Hu, S. H. (2016). Improvement of Engine Exhaust Particle Sizer (EEPS) size distribution measurement - II. Engine exhaust particles. *Journal of Aerosol Science*, *92*, 83–94. http://dx.doi.org/10.1016/j.jaerosci.2015.11.003.

Wu, C., Ng, W. M., Huang, J. X., Wu, D., & Yu, J. Z. (2012). Determination of elemental and organic carbon in PM2.5 in the pearl river delta region: Inter-Instrument (Sunset vs. DRI Model 2001 thermal/optical carbon analyzer) and inter-protocol comparisons (IMPROVE vs. ACE-Asia protocol). *Aerosol Science and Technology*, *46*(6), 610–621. http://dx.doi.org/10.1080/02786826.2011.649313.

Xue, J., Johnson, K. C., Durbin, T. D., Russell, R. L., Pham, L., Miller, W., & Jung, H. J. (2017). Very low particle matter mass measurement from light-duty vehicle. *Journal of Aerosol Science* (in preparation).

Xue, J., Li, Y., Quireos, D., Wang, X. L., Durbin, T. D., Johnson, K. C., & Jung, H. J. (2016b). Using a new inversion matrix for a fast-sizing spectrometer and a photo-acoustic instrument to determine suspended particulate mass over a transient cycle for light-duty vehicles. *Aerosol Science and Technology*, *50*, 1227–1238.

Xue, J., Li, Y., Wang, X. L., Durbin, T. D., Johnson, K. C., Karavalais, G., & Jung, H. J. (2015). Comparison of vehicle exhaust particle size distributions measured by SMPS and EEPS during steady-state conditions. *Aerosol Science and Technology*, *49*, 984–996.

Zervas, E., & Dorlhene, P. (2006). Comparison of exhaust particle number measured by EEPS, CPC, and ELPI. *Aerosol Science and Technology*, *40*(11), 977–984. http://dx.doi.org/10.1080/02786820600844093.